SINERGI Vol. 30, No. 2, June 2026: 411-420
http://publikasi.mercubuana.ac.id/index.php/sinergi
http://doi.org/10.22441/sinergi.2026.2.008

4×1 Quarter-Circle Notched array antenna with independent feeding for enhanced beam steering mechanism at C-band frequency

Tri Nur Arifin[1]*, Ganjar Febriyani Pratiwi[1], Erfiana Wahyuningsih[1], Arief Budi Santiko[2], Suisbiyanto Prasetya[2], Dian Rusdiyanto[3], Syah Alam[4], Yohanes Galih Adhiyoga[2]
[1]Electrical Engineering Study Program, Universitas Dian Nusantara, Indonesia
[2]Research Center for Telecommunication, National Research and Innovation Agency, Indonesia
[3]Department of Electrical Engineering, Universitas Mercu Buana, Indonesia
[4]Department of Electrical Engineering, Universitas Trisakti, Indonesia

Abstract
One of the main challenges in microstrip antenna design is achieving adaptive beam steering. Such mechanism cannot be realized using an antenna array with a corporate feeding technique; instead, each antenna element must be fed independently with specific phase differences to steer the beam as needed. This study aimed to develop a microstrip antenna that can adjust its beam direction by applying an independent feeding technique to a 4×1 microstrip array. The theoretical development focused on calculating the required progressive phase shifts for each antenna element to achieve target steering angles. The proposed beam steering mechanism was implemented using a power splitter and 6-bit digital phase shifters connected to each element of the novel array design. This configuration successfully achieved a beam steering range of approximately ±36°, resulting in a total coverage of about 72°. The simulation results showed that the 4×1 array antenna achieved a gain of 10.11 dBi. Fabrication and measurement of the single element antenna with Quarter-Circle Notched (QCN) elements worked at frequency of 3.47 – 3.57 GHz with a bandwidth of 100 MHz. The measured 4×1 QCN array demonstrated performance within 3.32 – 3.75 GHz, achieving a better bandwidth of 430 MHz. The results also demonstrated that optimal gain could be achieved by adjusting the element spacing. Furthermore, variations in phase shift had been shown to enhance the antenna's beam scanning capability beyond theoretical expectations.

Keywords:
Independent feeding;
Microstrip antenna array;
Quarter-circle notched patch;
Satellite communication;

Article History:
Received: May 28, 2025
Revised: October 22, 2025
Accepted: October 23, 2025
Published: June 4, 2026

Corresponding Author:
Tri Nur Arifin
Electrical Engineering Study Program, Universitas Dian Nusantara, Indonesia
Email: tri.nur.arifin@undira.ac.id

INTRODUCTION

In the era of modern communication technology, there is an increasing need for wireless communication systems with high performance. One technology that is currently being widely used in various antenna applications is phased array technology [1, 2, 3, 4]. This technology allows the antenna to adjust its beam direction to the desired angle through phase and amplitude modifications in the antenna feeding system. In addition, by utilizing a stacking configuration, the antenna gain can also be increased so this technology is suitable for applications that require high gain. Phased array antennas usually use a simple microstrip patch antenna type. Microstrip antennas have various advantages, such as small size, light weight, and low production costs, making them suitable for supporting phased array technology that is widely implemented in satellites, radars [5, 6, 7, 8], and mobile communication systems [9][10]. In satellite and cellular applications, the C-band frequency, which covers the frequency range of 3.7-4.2 GHz,

is often used because it is able to provide high bandwidth capacity and good performance in various weather conditions.

One of the main challenges in microstrip antenna design is the ability to perform adaptive beam steering. Beam steering technology allows an antenna to steer radio waves in a desired direction without the need to physically move the antenna. This is very important for improving the efficiency of signal transmission and reception, as well as reducing interference. However, the application of beam steering at C-Band frequencies has its own challenges, including feeding issues and controlling the phase and amplitude of each antenna element.

Various studies have been conducted to develop capabilities. Some studies focus on using analog/digital phase shifters [11, 12, 13], liquid crystal (LC) phase shifter [14, 15, 16], or waveguided phase shifter [17, 18, 19, 20] to control the phase of the signal given to each antenna element. For example, research by [12] developed an 8×1 rectangular array patch microstrip antenna at a frequency of 28 GHz using FR-4 using 3-bit phase shifter. They constructed a switchable feeding network capable of generating phase shifts of 45°, 90°, 135°, 180°, 225°, 270°, and 315°.

Research by [16] developed a Liquid Crystal Phase Shifter at a frequency of sub-6 GHz for phased array antenna. Phase shifting mechanism can be achieved by modulating the propagation constant loaded with a tunable equivalent capacitance controlled by a bias voltage. The proposed phase shifter operates at 4 GHz and enables beam steering in the elevation plane over a range of 0° to 20°.

In addition, research by [18] developed a novel phase shifter based on substrate-integrated waveguide (SIW) technology. A number of reconfigurable liquid metal (LM) vias were implemented as components to control the magnitude of the phase shift, where activating a greater number of LM vias results in a larger phase shift. Each LM via is capable of achieving a phase shift step ranging from 1° to 100°. However, many of these existing approaches encounter significant limitations related to system complexity, implementation cost, and performance constraints, particularly at C-band frequencies. Furthermore, the feeding mechanism in most array antenna designs is typically realized using an integrated feeding network with a single feed input port, designed for single polarization [21] or for dual polarization applications [22].

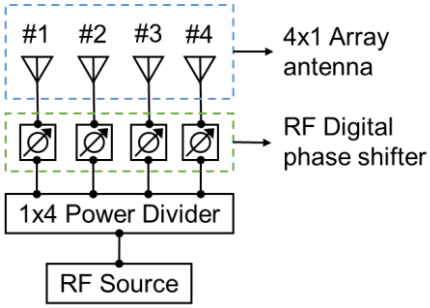

Figure 1. Electronic beam steering mechanism with independent feeding in the antenna array

This integrated feeding configuration inherently feeds all antenna elements with the same amplitude and phase characteristics, making it difficult to independently control each element. As a result, it becomes challenging to introduce variations in the feeding amplitude and phase required to realize effective beam steering. These gaps highlight the need for an alternative approach that allows independent control over each antenna element to achieve adaptive beam steering, especially within the C-band frequency range where such solutions remain scarce in the literature.

In this paper, the primary objective is to realize a microstrip antenna capable of steering its radiation pattern by employing an independent feeding approach on a 4×1 array designed for C-band operation. To this end, the study presents two principal contributions. First, it introduces an array antenna configuration utilizing Quarter-Circle Notched (QCN) elements; second, it implements an enhanced beam steering scheme that integrates a power splitter and 6-bit digital phase shifters, independently controlling each antenna element as illustrated in Figure 1. This approach offers more versatile solution for adaptive beam steering at C-band frequencies.

METHOD

In this study, two primary approaches were employed: antenna simulation and antenna measurement (Figure 2). Simulations were performed for the single-element antenna, sub-array antenna, and full antenna array. In addition to optimization, the simulation stage also included array synthesis to achieve the optimal antenna performance in attaining a specific scanning range based on the applied phase shifts. The single-element and sub-array antenna designs resulting from the simulations were subsequently fabricated for measurement. The comparison between the simulation and measurement results was used as the validation of this research.

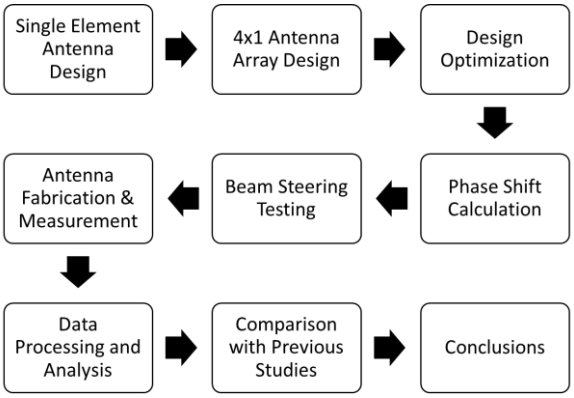

Figure 2. Research workflow for antenna array design and beam steering analysis

Numerical Simulation

Once the literature review had been conducted, the next step was to simulate the antenna design, which started from designing a single element antenna. The initial design of the single-element antenna was obtained by calculating the length and width of a rectangular microstrip antenna element by using Balanis formula as seen in (1) to (5) [23].

$$W = \frac{c}{2f_0\sqrt{\frac{(\varepsilon_r+1)}{2}}} \quad (1)$$

$$\varepsilon_{eff} = \frac{\varepsilon_r+1}{2} + \frac{\varepsilon_r-1}{2}\left[1+12\frac{h}{W}\right]^{-\frac{1}{2}} \quad (2)$$

$$L_{eff} = \frac{c}{2f_0\sqrt{\varepsilon_{eff}}} \quad (3)$$

$$\Delta L = 0.412h\frac{(\varepsilon_{eff}+0.3)(\frac{W}{h}+0.264)}{(\varepsilon_{eff}-0.258)(\frac{W}{h}+0.8)} \quad (4)$$

$$L = L_{eff} - 2\Delta L \quad (5)$$

This design was then further developed by incorporating quarter-circle cuts at two opposite corners. The quarter-circle notches were introduced as an alternative approach to achieve good impedance matching. The radius of the circular notches on both sides of the patch was optimized to improve the impedance matching performance. The results of the parametric study, as shown in Figure 3, revealed that increasing the radius led to better reflection coefficient, up to a saturation point at a radius of 10 mm.

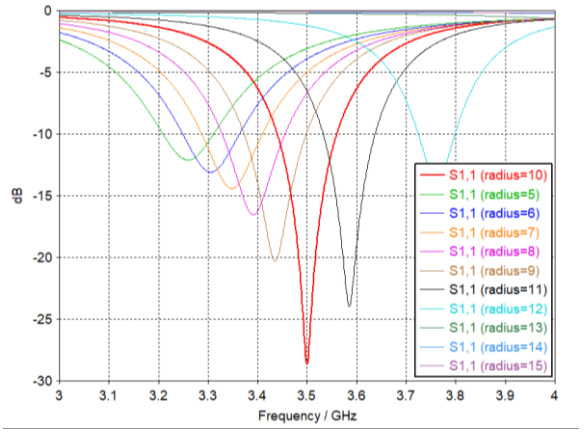

Figure 3. Parametric study of reflection coefficient for various radius of the quarter-circle cuts

The final optimized QCN antenna dimension is shown in Figure 4. The antenna was designed to work at a frequency of 3.5 GHz using an FR-4 substrate which has a dielectric constant of 4.3 and a dielectric loss of 0.0025. The antenna was fed directly through a coaxial probe with an impedance of 50 Ω. From the design, the antenna was then simulated to determine the working frequency, bandwidth, gain, radiation pattern, and beamwidth. To find out the working frequency of the antenna, the simulation was carried out on the reflection coefficient parameter (S_{11}). The smaller the value of S_{11} at a certain frequency, the better the antenna resonance at the frequency obtained. In addition, the antenna gain was also simulated to find out how much gain was generated by the antenna. The simulation results in terms of the gain of the single-element antenna compared to the array configuration can be seen in Figure 5.

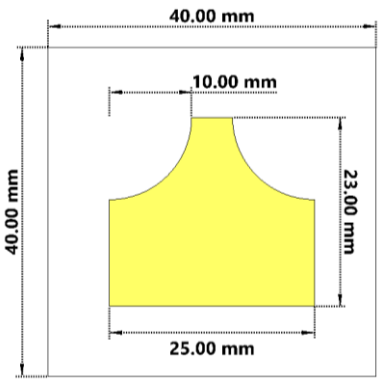

Figure 4. Optimized single-element QCN antenna design

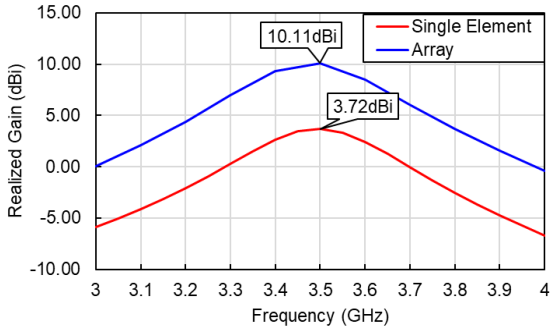

Figure 5. Comparison of gain of single-element QCN antenna and 4×1 array

Array Configuration

The next step after obtaining the appropriate single-element antenna characteristics was to arrange the antenna in an array configuration to achieve a wide scanning range with high antenna gain. In this research, the target was to achieve an antenna gain of greater than 20 dBi, with a 45° azimuth scan range. Array synthesis was performed to determine the required number of antenna elements and the optimum element spacing to achieve the highest possible gain. It was determined that 72 elements were needed, arranged in a 12×6 pattern. The results of the antenna design in the array configuration can be seen in Figure 6.

A parametric study was conducted on the element spacing to achieve the highest antenna gain, with the results shown in Figure 7. From that figure, it is evident that the maximum gain was achieved when the element spacing (d) was 73 mm, with a peak realized gain of 24.16 dBi.

Phase Shift Calculation

In a phased array system, the phase plays a crucial role in controlling the radiation direction of the antenna array. Therefore, in this study, independent feeding was implemented for each antenna element, making it possible to adjust the phase of each element individually. This approach enables easier control of the radiation pattern characteristics. The phase shift required for each element depends on the element spacing (d), the steering angle (θ), and the wavelength (λ) of the antenna, as shown in (6) [23].

$$\Delta\varphi = \frac{360^{\circ}.d.sin\,\theta_s}{\lambda} \quad (6)$$

Based on these calculations, the phase shifts that had to be applied to each element were obtained and set through phase shifters.

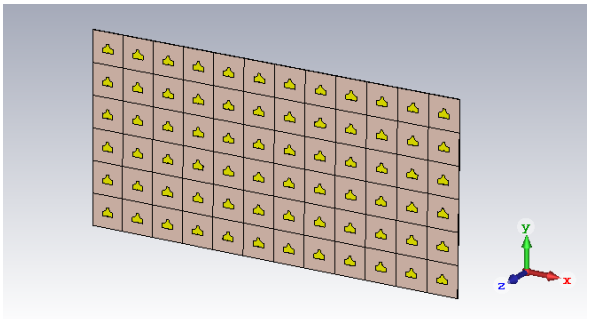

Figure 6. The design of 72-elements array antenna in 12×6 configuration

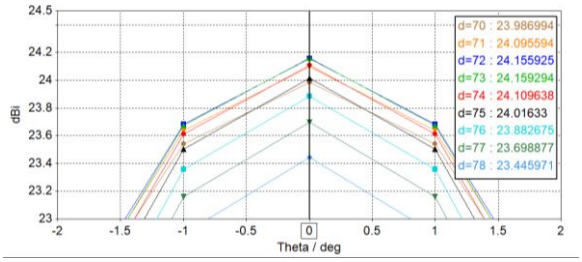

Figure 7. Realized gain for various element spacings in array antenna

A 6-bit digital phase shifter was used in this study, which provided a minimum resolution of 5.625°. As a result, the calculated phase shift had to be rounded to comply with the resolution of the phase shifter.

RESULTS AND DISCUSSION

Single-Element Measurement

The simulated antenna were then fabricated to further validate their performance through measurements. In this study, a single antenna was fabricated to validate the simulation results. The fabricated antenna is shown in Figure 8, while the measurement results of the S_{11} parameter on the single element antenna were shown in Figure 9.

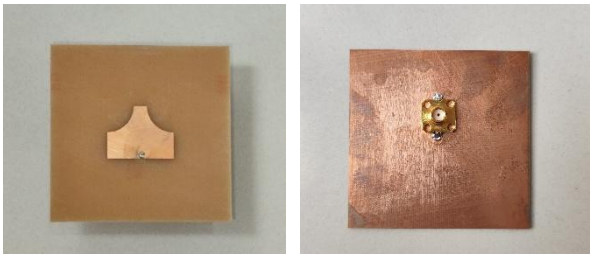

(a) (b)

Figure 8. Fabricated single-element QCN antenna: (a) front view; (b) back view with SMA connector attached in the ground plane

Figure 9 proves that the single-element QCN antenna worked at a frequency of 3.47 – 3.57 GHz with a bandwidth of 100 MHz. A slight frequency shift was observed between the simulation and fabrication results, attributed to the accuracy limitations of the fabrication process that led to dimensional deviations of the patch, as well as the effects of soldering between the SMA connector and the antenna patch.

4×1 Array Antenna Measurement

In this study, taking into account the availability of the antenna materials, a 4×1 sub-array was fabricated to represent the overall 12×6 array. The fabricated 4×1 antenna array can be seen in Figure 10. In Figure 10 (a), it can be seen that the QCN structure of the four elements has been printed on a substrate of the FR-4 material. It can also be seen in Figure 10 (b), that the SMA connector as an independent feed has been installed directly on the ground plane until it penetrates the substrate to the patch.

Validation was performed on the S_{11} and radiation pattern parameters for the antenna array. Based on the measurement results as shown in Figure 11, the proposed antenna can work at the expected frequency between 3.32 – 3.75 GHz with a bandwidth of 430 MHz. This result has significantly increased from the single-element antenna of only 100 MHz.

Radiation pattern measurements were also carried out to determine the shape of the radiation of the antenna. The measurement setup as shown in Figure 12 was applied using several measuring instruments such as a Keysight N9020A Spectrum Analyzer and Keysight N5183B Signal Generator as well as a SAS-571 Standard Gain Horn Antenna as a reference. Measurements were made using the far field method by placing the horn antenna at a far-field distance. The horn antenna was connected to a Signal Generator to generate an electromagnetic signal with 0 dB power. Opposite the horn antenna, the antenna under test (AUT) was placed in line perpendicular to the reference horn antenna. This AUT was connected to a spectrum analyzer to detect the electromagnetic signal received by the antenna. This process was repeated at all rotational angles with an angle variation of five degrees. From these measurements, the antenna's radiation pattern can be plotted as seen in Figure 13.

In Figure 13, it is evident that the antenna produced two main lobes that were opposite in direction with nearly identical radiation levels.

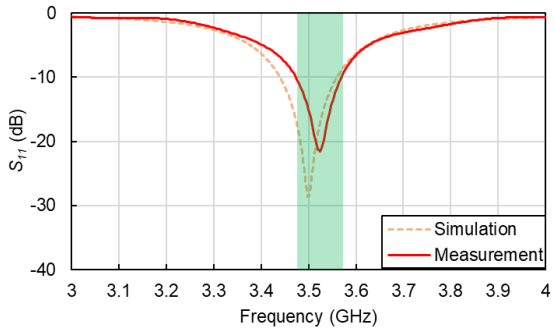

Figure 9. Simulation and measurement results of single-element QCN antenna reflection coefficient (S_{11})

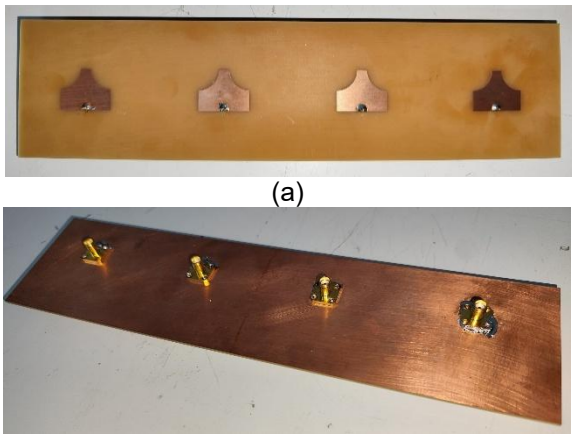

(a)

(b)

Figure 10. Fabricated 4×1 QCN array antenna: (a) front view, there are four radiating elements with QCN structure; (b) back view, there are SMA connectors to connect the cable with the antenna

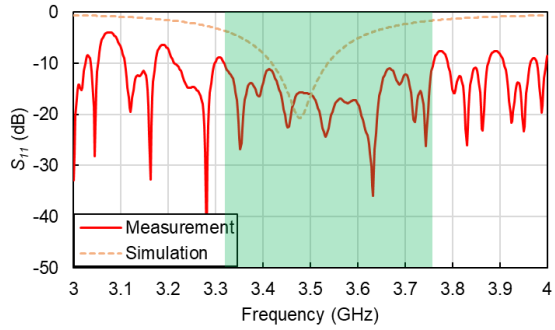

Figure 11. Measurement results of reflection coefficient (S_{11}) and VSWR parameters of 4×1 QCN array antenna

This is consistent with the findings of [24], where a PIN diode was used to control the reconfigurable antenna. Contrary, in this proposed antenna, the back lobe was not utilized as the main beam but rather as an enhancer when the antenna was supplemented with an additional reflector.

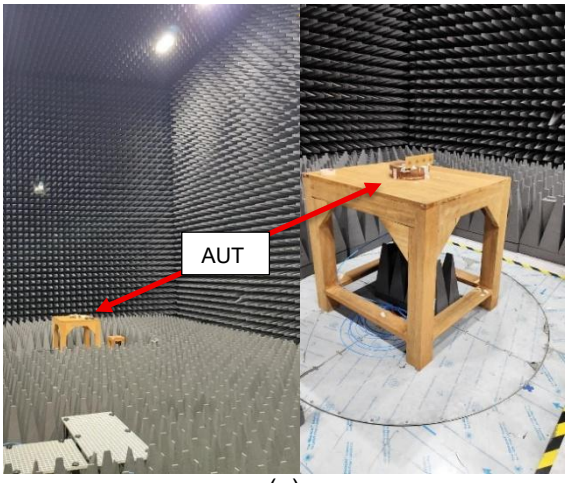

(a)

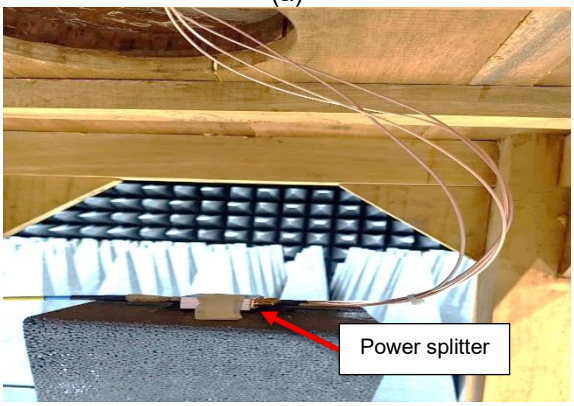

(b)

Figure 12. The radiation pattern measurement setup: (a) Placement of the AUT on a support table; (b) Position of the power splitter placed beneath the support table.

Beam Steering Performance

To evaluate the beam steering capability of the antenna array, an analysis was performed on the calculated phase shift values. These values were then adjusted according to the resolution of the phase shifter and subsequently applied to each antenna element. In this paper, the phase shifts were implemented on a 4×1 sub-array antenna. The beam results from several phase shift variations are presented in Table 1.

The parametric study presented in Table 1 provides clear evidence of the impact of varying the phase shift across the antenna elements on the beam direction, realized gain, and sidelobe level (SLL). Based on these results, the proposed combination of the Quarter-Circle Notched (QCN) structure with the 4×1 microstrip array and independent feeding technique enabled a wider beam steering range compared to theoretical calculations. Specifically, while the calculated phase shifts were designed to achieve main lobe steering from 0° up to 50°, the measured beam directions demonstrated an extended beam shift capability ranging from −36° to +36° (72° beam coverage). This enhanced steering range was primarily attributed to the unique electromagnetic properties of the QCN structure, which, when integrated with independent phase control, allows the antenna to achieve larger beam deviations than predicted by theory.

Moreover, the data also revealed a trade-off between steering angle, realized gain, and SLL, where increased beam deviation leads to slight reductions in gain and increased sidelobe levels. These findings confirm that the proposed design not only achieves effective beam steering through phase control but also extends the operational beam coverage beyond conventional expectations, establishing a significant advancement in microstrip array antenna performance.

Table 2 presents a comparison between the proposed antenna and existing beam-steering antenna designs. The proposed antenna achieved the widest beam scanning range (±36°) among the reported works, while employing only four radiating elements. A realized gain of 10.11 dBi was obtained, which is considered competitive for a compact structure operating in the C-band. Although higher gain values were reported in other designs, such as [25] and [26]. These typically involve a larger number of elements or increased structural complexity.

A significant advantage was observed through the combination of an independent feeding method, digital phase shifters, and quarter-circle notched (QCN) elements. Through this configuration, reconfigurable beam control was achieved without the use of time-delay lines or multilayer structures. As a result, the overall system complexity was reduced, and the design became more suitable for practical C-band applications.

CONCLUSION

This study demonstrates through experimental validation that both the single element and the array configurations meet the simulation results. The proposed single-element quarter-circle notched (QCN) antenna operates at approximately 3.47 – 3.57 GHz with a bandwidth of 100 MHz, and achieves a gain ranging from 2.4 to 3.72 dBi. The fabricated 4×1 QCN sub-array operates within the frequency range of 3.32 – 3.75 GHz, achieving a broader bandwidth of 430 MHz and a gain of 10.11 dBi.

Table 1. Beam Steering Results for Various Phase Shift Configurations

Desired mainlobe angle (°)	Calculated Phase Shift Angle (°)				Sim. mainlobe angle (°)	Realized Gain (dBi)	SLL (dB)
	Element #1	Element #2	Element #3	Element #4			
0	0	0	0	0	0	8.94	-12.70
10	0	67.5	129.375	196.875	-12	8.73	-10.80
20	0	129.375	258.75	28.125	-25	7.90	-2.80
25	0	157.5	320.625	118.125	-32	7.34	-1.00
26	0	163.125	331.875	135	-33	7.23	-0.70
27	0	174.375	343.125	157.5	-35	7.08	-9.40
28	0	180	354.375	174.375	-36	6.96	-9.30
29	0	185.625	5.625	191.25	36	6.99	-9.30
30	0	191.25	16.875	208.125	34	7.11	-9.40
40	0	241.875	123.75	11.25	23	8.11	-3.90
50	0	286.875	219.375	146.25	14	8.68	-9.70
60	0	326.25	292.5	264.375	6	8.90	-11.90
70	0	354.375	348.75	343.125	1	8.94	-12.60

Table 2. Comparison between the proposed antenna and related works

Ref.	Freq. (GHz)	Beam Scanning Range (°)	Realized Gain (dBi)	No. of Element	Feeding Technique
[27]	26.0	±34°	9.30	4	reconfigurable 1-bit phase shifter
[28]	27.0	±33°	9.16	4	overlapped apertures
[25]	8.0	-24° to 36°	20.9	16	quadrature based feeding
[29]	10.0	±30°	19.10	3	metasurface lens array
[30]	27.5	±25°	10.80	4	time delay transmission lines
[31]	15.0	-13° to 28°	12.72	N/A	air-filled SIW
[32]	4.5	±30°	14.31	8	combined single-layer transmitarray
[33]	3.5	±32°	2.40	4	meandered lines with dual-stub-based filter
[26]	20.0	±20°	13.46	49	hybrid transmitarray unit cell
This work	3.53	±36°	10.11	4	independent feed phase shifter

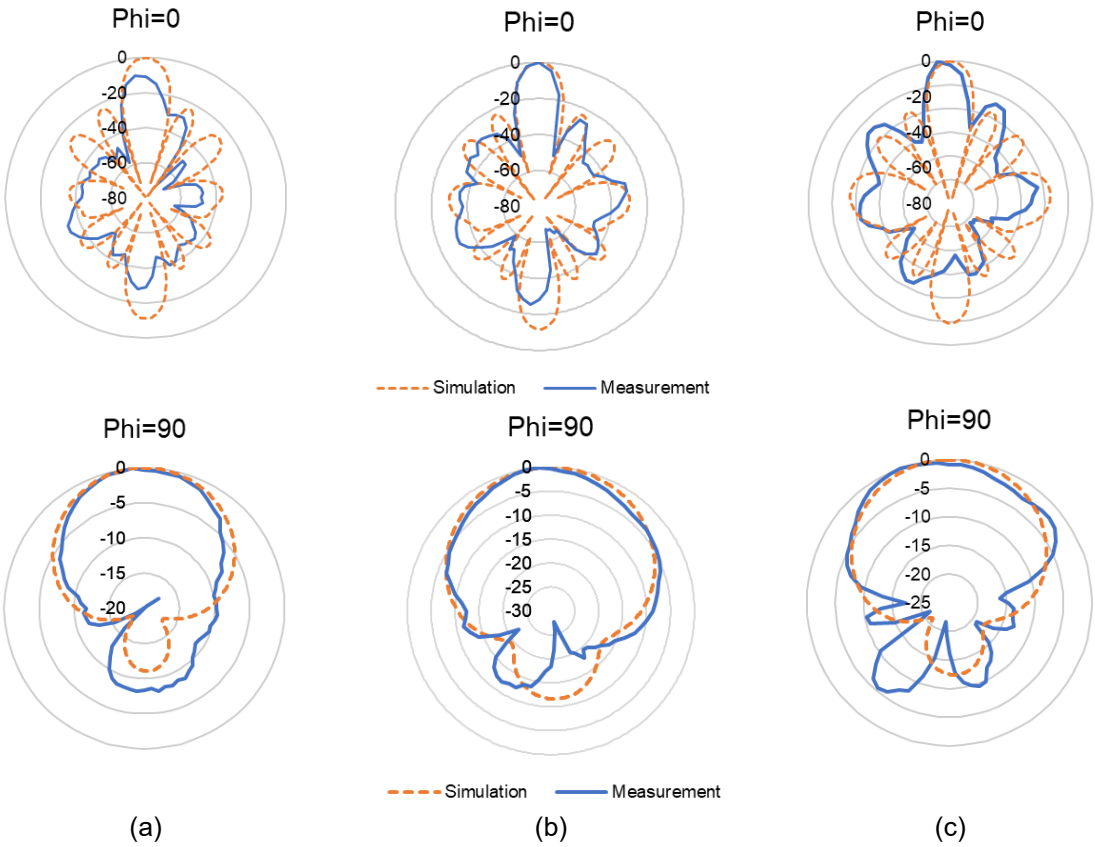

Figure 13. Measurement results of 4×1 QCN array antenna radiation pattern at: (a) 3.45 GHz; (b) 3.53 GHz; and (c) 3.63 GHz

The application of an independent feeding technique with digital phase shifters and the use of QCN elements enhances the beam steering capability to approximately ±36°, which gives a total beam coverage of about 72°. This improvement over theoretical calculations based on the array factor confirms that the proposed combination effectively overcomes the limitations of conventional feeding systems and achieves better adaptive beam steering performance.

ACKNOWLEDGMENT

This work was supported by the Directorate General of Higher Education, Research, and Technology in terms of Penelitian Dosen Pemula (PDP) under Grant No: 11/135/H-SPK/VI/2024. The author would also like to thank the Institute for Research and Community Service (LRPM), Universitas Dian Nusantara, and the Research Center for Telecommunication, National Research and Innovation Agency (BRIN) for the research facility support. Additionally, the author extends gratitude for the use of AI tools (Microsoft Copilot version 1.24123.47.0), which assisted in improving the quality of the English language in this manuscript.

REFERENCES

[1] A. H. Aljuhani, T. Kanar, S. Zihir, and G. M. Rebeiz, "A 256-Element Ku-Band Polarization Agile SATCOM Transmit Phased Array With Wide-Scan Angles, Low Cross Polarization, Deep Nulls, and 36.5-dBW EIRP per Polarization," *IEEE Trans. Microw. Theory Tech*., vol. 69, no. 5, pp. 2594–2608, 2021, doi: 10.1109/TMTT.2021.3053293.

[2] A. H. Aljuhani, T. Kanar, S. Zihir, and G. M. Rebeiz, "A 256-Element Ku-Band Polarization Agile SATCOM Receive Phased Array With Wide-Angle Scanning and High Polarization Purity," *IEEE Trans. Microw. Theory Tech.,* vol. 69, no. 5, pp. 2609–2628, May 2021, doi: 10.1109/TMTT.2021.3056439.

[3] G. Gültepe and G. M. Rebeiz, "A 256-Element Dual-Beam Polarization-Agile SATCOM Ku-Band Phased-Array With 5-dB/K G/T," *IEEE Trans. Microw. Theory Tech*., vol. 69, no. 11, pp. 4986–4994, 2021, doi: 10.1109/TMTT.2021.3097075.

[4] X. Luo et al., "A Scalable Ka-Band 1024-Element Transmit Dual-Circularly-Polarized Planar Phased Array for SATCOM Application," *IEEE Access*, vol. 8, pp. 156084–156095, 2020, doi: 10.1109/ACCESS.2020.3019174.

[5] Y.-E. Chi, J. Park, and S.-O. Park, "Hybrid Multibeamforming Receiver With High-Precision Beam Steering for Low Earth Orbit Satellite Communication," *IEEE Trans. Antennas Propag*., vol. 71, no. 7, pp. 5695–5707, 2023, doi: 10.1109/TAP.2023.3277195.

[6] Z. Zhang, M. Gao, M. M. Honari, J. Wu, J. H. Booske, and N. Behdad, "A Wideband, 1-bit, Electronically Reconfigurable Phase Shifter for High-Power Microwave Phased-Array Applications," *IEEE Transactions on Plasma Science*, vol. 51, no. 7, pp. 1849–1861, 2023, doi: 10.1109/TPS.2023.3246729.

[7] P. Yu and D. Zhao, "Design Considerations for Wideband Hybrid Large-Scale Antenna Array and Implementation of a 5–23-GHz CMOS True-Time-Delay Circuit," *IEEE Transactions on Circuits and Systems II: Express Briefs*, vol. 71, no. 1, pp. 26–30, 2024, doi: 10.1109/TCSII.2023.3298482.

[8] L. Polo-López et al., "Mechanically Reconfigurable Linear Phased Array Antenna Based on Single-Block Waveguide Reflective Phase Shifters With Tuning Screws," *IEEE Access*, vol. 8, pp. 113487–113497, 2020, doi: 10.1109/ACCESS.2020.3003193.

[9] Y. Rahayu, Y. B. Pradana, and Y. Yamada, "Dual-band frequency reconfigurable 5G microstrip antenna," *Sinergi (Indonesia),* vol. 27, no. 1, pp. 81–88, 2023, doi: 10.22441/sinergi.2023.1.010.

[10] P. Haryanto, D. W. Astuti, M. Alaydrus, A. Firdausi, D. Rusdiyanto, and H. A. Majid, "An ultra-broadband microstrip antenna using a triple dumbbell-shaped defected ground structure," *Sinergi (Indonesia),* vol. 30, no. 1, pp. 79–90, 2026, doi: 10.22441/sinergi.2026.1.008.

[11] L. Yin, P. Yang, Y. Gan, F. Yang, S. Yang, and Z. Nie, "A Low Cost, Low in-Band RCS Microstrip Phased-Array Antenna With Integrated 2-bit Phase Shifter," *IEEE Trans. Antennas Propag*., vol. 69, no. 8, pp. 4517–4526, 2021, doi: 10.1109/TAP.2020.3048575.

[12] M. N. Uddin, M. N. A. Tarek, M. K. Islam, and E. A. Alwan, "A Reconfigurable Beamsteering Antenna Array at 28 GHz Using a Corporate-Fed 3-Bit Phase Shifter," *IEEE Open Journal of Antennas and Propagation*, vol. 4, pp. 126–140, 2023, doi: 10.1109/OJAP.2023.3237882.

[13] Y. Shang, Q. Zeng, W. Cui, X. Wang, and G. Zheng, "Design of Pattern Reconfigurable Patch Antenna Array Based on Reflective Phase-Shifter," *Int. J. Antennas Propag.*, vol.

2022, no. 1, p. 2803285, Jan. 2022, doi: https://doi.org/10.1155/2022/2803285.
[14] D. Wang, E. Polat, H. Tesmer, R. Jakoby, and H. Maune, “A Compact and Fast 1×4 Continuously Steerable Endfire Phased-Array Antenna Based on Liquid Crystal,” *IEEE Antennas Wirel. Propag. Lett.*, vol. 20, no. 10, pp. 1859–1862, 2021, doi: 10.1109/LAWP.2021.3096035.
[15] J. Liu et al., “Circularly Polarized High-Gain K-Band Liquid Crystal Phased Array Antenna,” *IEEE Trans. Antennas Propag.*, vol. 72, no. 9, pp. 7341–7346, 2024, doi: 10.1109/TAP.2024.3431193.
[16] M. A. Panahi, L. Yeung, M. Hedayati, and Y. E. Wang, “Sub-6 GHz High FOM Liquid Crystal Phase Shifter for Phased Array Antenna,” *IEEE Journal of Microwaves*, vol. 2, no. 2, pp. 316–325, 2022, doi: 10.1109/JMW.2022.3152208.
[17] S. Alkaraki, Q.-W. Lin, J. R. Kelly, Z. Wang, and H. Wong, “Phased Array Antenna System Enabled by Liquid Metal Phase Shifters,” *IEEE Access*, vol. 11, pp. 96987–97000, 2023, doi: 10.1109/ACCESS.2023.3308068.
[18] S. Alkaraki et al., “10-GHz Low-Loss Liquid Metal SIW Phase Shifter for Phased Array Antennas,” *IEEE Trans. Microw. Theory Tech.*, vol. 71, no. 11, pp. 5045–5059, 2023, doi: 10.1109/TMTT.2023.3308160.
[19] D. Sánchez-Escuderos, J. I. Herranz-Herruzo, M. Ferrando-Rocher, and A. Valero-Nogueira, “Mechanical phase shifter in gap-waveguide technology,” in *2020 14th European Conference on Antennas and Propagation (EuCAP)*, 2020, pp. 1–5. doi: 10.23919/EuCAP48036.2020.9135719.
[20] M. Nickel et al., “Ridge Gap Waveguide Based Liquid Crystal Phase Shifter,” *IEEE Access*, vol. 8, pp. 77833–77842, 2020, doi: 10.1109/ACCESS.2020.2989547.
[21] D. Rusdiyanto, D. W. Astuti, M. Muslim, S. Alam, and Y. G. Adhiyoga, “Design of 2x2 Wide Bandwidth MIMO Antenna For LTE And 5G Sub-6GHz,” *Journal of Informatics and Telecommunication Engineering*, vol. 5, no. 2, pp. 225–238, 2022, doi: 10.31289/jite.v5i2.5699.
[22] S. Abdi, M. Mohammadpour, and M. Hatam, “A Dual-Polarized Slotted Waveguide Array Antenna with High Isolation and Low Cross-Polarization,” *Iranian Journal of Science and Technology, Transactions of Electrical Engineering*, Aug. 2025, doi: 10.1007/s40998-025-00848-9.
[23] C. A. Balanis, “Rectangular Cross-Section Waveguides and Cavities,” in *Balanis’ Advanced Engineering Electromagnetics*, Third Edition., Wiley, 2023, ch. 8, pp. 365–478. doi: https://doi.org/10.1002/9781394180042.ch8.
[24] Y. Rahayu, Y. B. Pradana, and Y. Yamada, “Dual-band frequency reconfigurable 5G microstrip antenna,” *Sinergi (Indonesia)*, vol. 27, no. 1, pp. 81–88, Jan. 2023, doi: 10.22441/sinergi.2023.1.010
[25] A. B. Patwary and I. Mahbub, “4×4 UWB Phased Array Antenna With >51° Far-Field Scanning Range for Wireless Power Transfer Application,” *IEEE Open Journal of Antennas and Propagation*, vol. 5, no. 2, pp. 354–367, 2024, doi: 10.1109/OJAP.2023.3349358.
[26] M. Wellandari, A. Firdausi, U. Umaisaroh, and M. Alaydrus, “Design of Hybrid Element Transmitarray Antenna with Beamforming at Millimeter-wave Frequency,” in *2021 International Conference on Radar, Antenna, Microwave, Electronics, and Telecommunications (ICRAMET)*, 2021, pp. 74–78. doi: 10.1109/ICRAMET53537.2021.9650461.
[27] Y. Wang, F. Xu, Y.-Q. Jin, and Z. Du, “Low-Cost Reconfigurable 1 bit Millimeter-Wave Array Antenna for Mobile Terminals,” *IEEE Trans. Antennas Propag.*, vol. 70, no. 6, pp. 4507–4517, 2022, doi: 10.1109/TAP.2022.3140508.
[28] H. Li, Y. Li, L. Chang, W. Sun, X. Qin, and H. Wang, “A Wideband Dual-Polarized Endfire Antenna Array With Overlapped Apertures and Small Clearance for 5G Millimeter-Wave Applications,” *IEEE Trans. Antennas Propag.*, vol. 69, no. 2, pp. 815–824, 2021, doi: 10.1109/TAP.2020.3016512.
[29] R. Xu and Z. N. Chen, “A Compact Beamsteering Metasurface Lens Array Antenna With Low-Cost Phased Array,” *IEEE Trans. Antennas Propag.*, vol. 69, no. 4, pp. 1992–2002, 2021, doi: 10.1109/TAP.2020.3026905.
[30] R. W. Asfour, S. K. Khamas, and E. A. Ball, “Design and Measurements of Circularly Polarized Millimeter-Wave Phased Array Antenna Using Time Delay Transmission Lines,” *IEEE Access*, vol. 11, pp. 122016–122028, 2023, doi: 10.1109/ACCESS.2023.3329088.
[31] R. Hong, J. Shi, D. Guan, W. Cao, and Z. Qian, “Wideband and Low-Loss Beam-Scanning Circularly Polarized Antenna Based on Air-Filled SIW,” *IEEE Antennas Wirel. Propag. Lett.*, vol. 20, no. 7, pp. 1254–1258, 2021, doi: 10.1109/LAWP.2021.3077263.

[32] D. E. Serup, G. F. Pedersen, and S. Zhang, "Combined Single-Layer K-Band Transmitarray and Beamforming S-Band Antenna Array for Satcom," *IEEE Open Journal of Antennas and Propagation*, vol. 3, pp. 1134–1140, 2022, doi: 10.1109/OJAP.2022.3203253.

[33] S. Islam, M. Zada, and H. Yoo, "Highly Compact Integrated Sub-6 GHz and Millimeter-Wave Band Antenna Array for 5G Smartphone Communications," *IEEE Trans. Antennas Propag*., vol. 70, no. 12, pp. 11629–11638, Dec. 2022, doi: 10.1109/TAP.2022.3209310.